Progress in Nuclear Energy 109 (2018) 223–232

Contents lists available at ScienceDirect

Progress in Nuclear Energy

journal homepage: www.elsevier.com/locate/pnucene

A lumped parameter modelling of particle generation from Na-pool fires in SFR containments

L.E. Herranz[a], M. Garcia[a,b,*], M.P. Kissane[c], C. Spengler[d]

[a] CIEMAT, Unit of Nuclear Safety Research, Av. Complutense, 40, 28040 Madrid, Spain
[b] Universidad Politécnica de Madrid (UPM), Energy Engineering Department, José Gutierrez Abascal, 2, 28006 Madrid, Spain
[c] Nuclear Safety Technology and Regulation Division, OECD Nuclear Energy Agency (NEA), 46 quai Alphonse Le Gallo, 92100 Boulogne-Billancourt, France
[d] Gesellschaft für Anlagen-und Reaktorsicherheit (GRS), gGmbH, Cologne, Germany

ARTICLE INFO

Keywords:
Sodium-cooled fast reactor
In-containment source term
Sodium-pool fire
Particle generation model
Correlations

ABSTRACT

Modelling of sodium-evaporation and formation of sodium-oxide aerosols from a sodium-pool fire is of fundamental importance for the assessing of the radiological consequences in Sodium-cooled Fast Reactors severe accidents. This paper summarizes the derivation of a simple model to estimate the amount and size of particles being generated from Na-pool fires and its performance assessment, once implemented in an integral severe accident tool (ASTEC-Na), against available large-scale separate effect tests. The model has been transposed in analytical correlations which implementation in lumped-parameter severe accident codes is straightforward. According to the comparisons to data set, the correlations do not adversely impact the code estimates with respect to other more empirical alternative approaches and, in addition, the correlations remove any need of user-defined ad-hoc parameters in the input deck concerning Na-based particles behaviour, as other alternates do. Regarding code behaviour, the model predictions yield the same order of magnitude both in terms of suspended aerosol concentration and diameter as data and capture the reliable measured data trends.

1. Introduction

In case of a severe accident in a Sodium Fast Reactor (SFR), sodium-based particles may be considered as key carriers of the radiological and chemical threat of any potential release to the environment. Their formation from sodium (Na) pool and/or spray fires strongly depends on processes such as sodium vaporization, chemical reactions with the surrounding gas, nucleation/condensation and primary particle agglomeration. Therefore, a full-scope risk assessment of SFRs would require analytical tools in which a suitable modelling of Na-based particle generation is properly accounted for, which points to the need to build a multidisciplinary model coupling thermal hydraulics, chemical reactivity of Na species and compounds and particle dynamics (Yamaguchi and Tajima, 2009). The final outcomes of any Na-based aerosol generation model are particle concentration, size and composition.

Since the early 70s last century, Na burning and Na-based aerosol behaviour and their chemical composition have been the subject of experimental research projects conducted in facilities like PLUTON (Lhiaubet et al., 1990) and JUPITER (Malet et al., 1990) in France, CSTF in the USA (Hilliard et al., 1977, 1979; McCormack et al., 1978; Souto et al., 1994), FAUNA in Germany (Cherdron et al., 1985, 1990, Cherdron and Jordan, 1980, 1983) and ATF in India (Baskaran et al., 2011; Subramanian et al., 2009; Subramanian and Baskaran, 2007). As for pool-fire modelling, Beiriger et al. (1973) achieved a major milestone in the field by developing the SOFIRE code, a tool focused on fire energetics to model the whole SFR severe accident scenario by assuming that $Na-O_2$ reactions take place on the pool surface (i.e., surface approach). Later on, Sagae and Suzuoki (1985), inspired by Newman (1983), developed an alternative model based on Na diffusion to the gas atmosphere from a hot pool (over 800 °C) and its subsequent reactions of Na and O_2 in gas phase (flame sheet approach). Miyake et al. (1991), Lee and Choi (1997), or more recently Yamaguchi and Tajima (2003) or Takata et al. (2003) included the vapour-phase sodium-combustion modelling in several combustion codes (SPM, SOPA, SPHINCS or AQUA-SF code respectively).

The above mentioned computer codes have mostly focused on pool-fire energetics and thermal-hydraulics (Murata et al., 1993) so that particle modelling has received much less attention and usually built on major hypotheses not thoroughly proved. The SOFIRE code, for

* Corresponding author. CIEMAT, Unit of Nuclear Safety Research, Av. Complutense, 40, 28040 Madrid, Spain.
E-mail addresses: luisen.herranz@ciemat.es (L.E. Herranz), monica.gmartin@ciemat.es (M. Garcia), Martin.KISSANE@oecd.org (M.P. Kissane), Claus.Spengler@grs.de (C. Spengler).

https://doi.org/10.1016/j.pnucene.2018.08.015
Received 2 March 2018; Received in revised form 21 August 2018; Accepted 23 August 2018

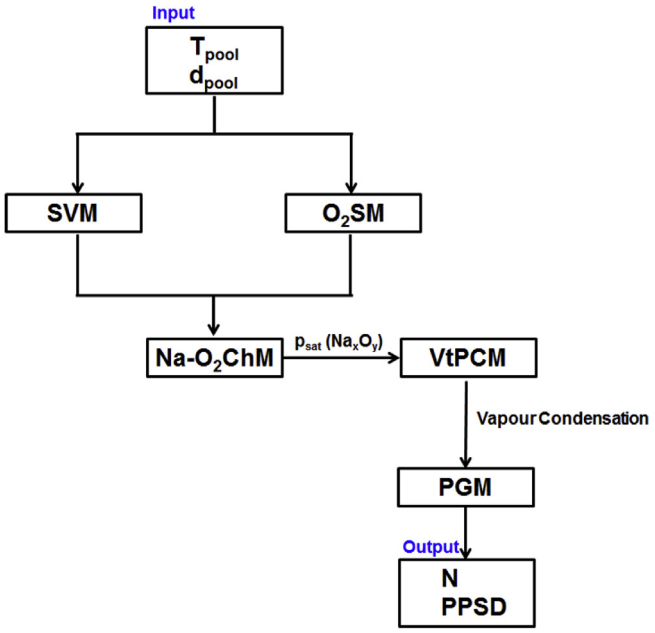

Fig. 1. PG model diagram.

example, assumes that all sodium oxides (Na_xO_y) produced become particles of a given size with no specific consideration of particle formation kinetics or primary-particle size. The CONTAIN-LMR code (Murata et al., 1993), which is heavily inspired by SOFIRE regarding Na combustion, requires the user to set a particle seed size and to introduce a number of parameters that heavily control both Na-based particle generation and subsequent behaviour (Herranz et al., 2017).

Due to the attention that Source Term is being given in the frame of Gen. IV SFR (Girault et al., 2015, 2017) designs to achieve better assessments of SFR potential risks and/or more efficient development of engineered safety features, an *ad-hoc* particle generation model from Na-pool fires has been built by Garcia et al. (2016). The model consists of a suite of individual models for Na vaporization (diffusion layer approach), O_2 transport by air natural circulation (3D flow pattern modelling), $Na-O_2$ chemical reactions (instantaneous reactions and energy of reaction) and vapour-to-particle conversion of Na-oxides (i.e., nucleation and/or condensation). Fig. 1 shows a simplified flowchart of the coupling of individual models. By characterizing sodium pools through temperature and diameter, a Sodium Vaporization Model (SVM) calculates the vaporized Na from the surface. Highly turbulent conditions foreseen in the close vicinity of the sodium reaction zone together with the O_2 supply to the reaction region require a 3D Computational Fluid Dynamics (CFD) approach to be used. By using FLUENT (ANSYS Inc., 2008), the O_2 natural circulation and the $Na-O_2$ chemical reactions are modelled (O_2 Supply Model, O_2SM; $Na-O_2$ Chemical Model, $Na-O_2$ChM). Then, a Vapour-to-Particle Conversion model (VtPCM) calculates particle generation by homogeneous nucleation and particle growth by condensation of the formed sodium oxides. As a result, the Particle Generation (PG) model produces the total number of generated particles (N) and the Primary Particle Size Distribution (PPSD) during an in-containment sodium pool fire. The authors partially validated the model with data from Newman and Payne (1978) and showed a consistent model response in terms of burning rate. However, as stated above, such an agreement requires capturing the 3D natural circulation that feeds the $Na-O_2$ reaction layer and the associated turbulence foreseen right above such a reaction region.

The current international trend in the development of SFR severe accident codes is to take advantage of the commonalities with LWR ones, so that the main code architecture and programming is adopted, and just modifications to account for those phenomena that are specific of SFRs are to be included. This was, for example, the strategy in the European JASMIN project of the 7th Framework Programme of EURATOM. Nevertheless, this approach is not free of drawbacks, like the fact that the description of some of those specific phenomena might require variables not included in the original code. In other words, once a model describing a phenomenon is developed and validated, it might still require some further work to make it compatible with the code structure and language. This is the main focus of the present paper: transposing the PG formulation introduced above into a form ready to be implemented in any lumped-parameter code to be used for SFR severe accident analysis such as MELCOR/CONTAIN-LMR (Louie and Humphries, 2016) and/or ASTEC-Na (Girault et al., 2015, 2017). Finally the performance of the ASTEC-Na code with the proposed correlations implemented is analysed by comparing its predictions with some of the most credited experiments on aerosol behaviour in SFR containments.

2. Zero-D particle generation modelling

As mentioned above, particle generation from a Na-pool fire is associated with substantial gradients of temperature, Na_xO_y vapours and oxygen concentrations as well as turbulent agitation in the region right over the thin reaction layer set up next to the pool surface. Thus, the use of a 3D approach to capture the entire picture of particle generation seems to be recommendable. Nevertheless, using 3D computational fluid dynamics in analysis of Beyond Design Basis Accidents (BDBAs) at present is unsuitable, due to the lack of validation of these tools in SFR accident conditions, and impractical, since the necessary computing resources and the number of scenarios to be explored would render this approach too onerous. Therefore, a zero-D (lumped) approach is to be developed based on the work by Garcia et al. (2016).

In order to turn the chosen 3D model into a consistent 0D version, some qualitative criteria have been adopted:

- The 0D response to major environmental variables (i.e., pool temperature, oxygen concentration, over-pool gas velocity and composition, etc.) should follow the same trends shown by the original 3D model;
- The quantitative deviations of the 0D predictions with respect to the 3D estimates should be within the uncertainty range of the latter in the main output variables of the model (i.e., particle generation rate and primary-particle size distribution);
- The final formulation of the 0D model should be compatible with architecture and variables available in integral lumped-parameter codes to be used for SFR severe accident analyses (i.e., MELCOR-Na and/or ASTEC-Na).

2.1. Zero-D model

2.1.1. Fundamental equations

In addition to the qualitative criteria introduced above, the 0D adaptation of the PG model is based on the preservation of the total number of particles formed in the active nucleation volume (i.e., the region over the pool in which Na-oxides are supersaturated) in the 3D model, i.e.,:

$$N_{3D} = \sum_i \left(\int_{\Delta t} J_i^{CNT}\left(T_i, p_{v_i}\right)\cdot dt \right)\cdot v_i \equiv N_{0D} = \left(\int_{\Delta t} J^{CNT}\left(\overline{T}, \overline{p}_v\right)\cdot dt \right)\cdot V_{PG} \quad (1)$$

In Eqn. (1), the number of generated particles (N_{3D}) in the active volume is given by the integration over time of the nucleation rate in all the cells forming the active volume (summation running over subindex i). As shown at the right side of the equation, the 0D approximation requires a characteristic nucleation rate that keeps the major Classical Nucleation Theory dependencies and relies on average gas properties

$(\overline{T}, \overline{p_v})$ of the entire active volume (Becker and Döring, 1935; Farkas, 1927; Zeldovich, 1942):

$$N_{0D} = \left(\int_{\Delta t} \left[\left(\frac{2\sigma}{\pi\, m_1} \right)^{1/2} \cdot v_1 \cdot \overline{N}_1^2 \cdot \exp\left(-\frac{16\pi}{3} \frac{v_1^2 \sigma^3}{(k\overline{T})^3 (\ln \overline{S})^2} \right) \right] \cdot dt \right) \cdot V_{PG} \quad (2)$$

$$\overline{T} = \frac{1}{V_{PG}} \sum T_i \cdot v_i \quad (3)$$

$$\overline{p_v} = \frac{1}{V_{PG}} \sum p_{v_i} \cdot v_i \quad (4)$$

$$\overline{S} = \frac{\overline{p_v}}{p_{sat}(\overline{T})} \quad (5)$$

As in Eqn. (2), the critical particle size of the 0D adaptation (i.e., the minimum particle size to start up nucleation) is calculated for average gas conditions:

$$d_{0D} = \frac{2\sigma v_1}{k\overline{T} \ln \overline{S}} \quad (6)$$

Then, primary particle growth by later condensation is accounted for by vapour condensation on the primary particles formed by homogeneous nucleation (Garcia et al., 2016).

2.1.2. The model assessment

Given the absence of an *ad-hoc* experimental database on particle generation from sodium pool fires, a theoretical-case matrix has been set up as an engine to build an analytical database resulting from the 3D model running under the outlined scenarios. The cases have been characterized by variables physically related to the governing phenomena in the anticipated scenario: pool diameter (from 0.1 m to 10.0 m) as a characteristic system dimension for natural convection over the pool; pool temperature (from 850 K to 1100 K) as the main driver for the Na evaporation from the pool; and oxygen concentration (from 21% down to 1%) as a reactant which might potentially limit the conversion of Na into Na_xO_y. Table 1 synthesizes the discrete values selected to build up a total of 200 cases.

Some of the cases calculated were eventually screened out due to different reasons. Cases with 1% O_2 have been dropped from the matrix because homogeneous nucleation conditions are not met (a total of 40 cases dismissed). A check of mass balance consistency has been conducted to ensure that the 3D model does not artificially produce particles richer in Na than what the pool vaporization rate would allow; this second condition entailed dropping 28 more cases from the matrix. Thus, in total the analytical-case matrix consisted of 132 cases.

The calculated total number of particles by the PG model (N_{3D}) versus the total number of generated particles from the 0D adaptation (N_{0D}) for 132 scenarios is shown in Fig. 2 (some areas of the plot have been amplified for easier observation). As observed, the total number of particles ranged between 10^{18} and 10^{24} for any of the O_2 concentrations considered, so that a broad interval of particle number has resulted from the cases considered in the matrix. It is worth noting that both approaches agreed in the order of magnitude of particles formed, experiencing an average deviation of around 4% (never exceeding 15%).

In the 0D PG model, all the particles are generated under the same average conditions for a given scenario so that the growth rate is identical for all the particles. This prevents a strict quantitative comparison between the 3D approach and the 0D one, but a qualitative comparison still makes sense. Fig. 3 shows that primary particle size extends from around $7.0{\cdot}10^{-10}$ m to $1.2{\cdot}10^{-9}$ m in both approaches despite the absence of distributions in the 0D model. In the PG model (Fig. 3a), primary particle size is calculated by considering a single burst of homogeneous nucleation (critical size). From this point on, particle growth is controlled by condensation onto primary particles, which in turn depends on boundary conditions. Oxygen concentration has been noted to have a noticeable impact in the particle size distribution: the higher the oxygen concentration, the higher the particle number and the smaller the particle diameter. Namely, high oxygen concentration enhances formation of Na_xO_y so that Na_xO_y vapour pressure increases and nucleation occurs at smaller critical particle size. Consistently with this, the 0D approximation also estimates smaller sizes for higher O_2 concentrations (Fig. 3b).

Table 1
Tests matrix.

Key Variable	Range	Cases
Pool diameter (m)	0.1–10	0.1, 0.2, 0.5, 1.0, 2.0, 5.0, 7.5, 10.0
Pool temperature (K)	850–1100	850, 900, 950, 1000, 1100
O_2 content (%)	1–21	1, 5, 10, 15, 21

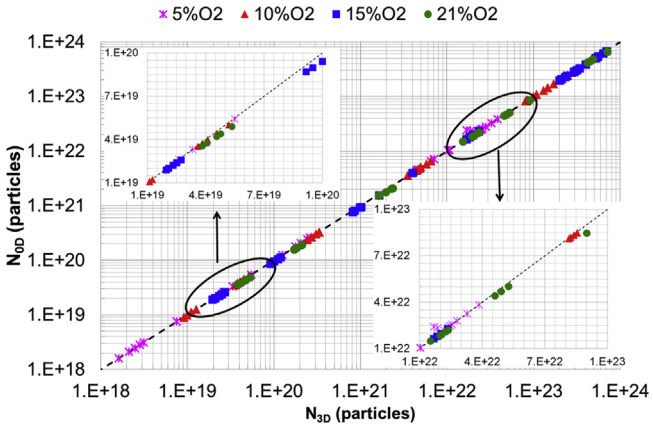

Fig. 2. N_{0D} vs N_{3D}.

In summary, the 0D model adaptation has been shown to succeed in meeting the two quantitative criteria set in terms of number of particles and primary particle size.

2.2. Zero-D correlations

Some of the variables embedded in Eqns. (1) and (5) might not be available in lumped parameter codes used for severe accident analysis of SFRs (N_1 or $\overline{S}$, for example). By exploring the sensitivity of the model to variables governing dominant processes (as stated in Table 1), the physical consistency of the 0D model may be confirmed and the key model trends revealed. They will be the pillars for the 0D correlation proposed below, the architecture of which will allow a straightforward implementation within severe accident system codes, like ASTEC-Na.

Figs. 4 and 5 present the N_{0D} model trends with Na vaporization rate and oxygen fraction. Fig. 4 shows a sound linear trend (drawn in black) of the number of particles with the Na-vaporization rate, although there is a substantial scattering (1- 2 orders of magnitude) at any Na-vaporization rate that accounts for other variables influence. Such an increase is what is expected since the more Na vapour is made available, the higher the number of particles might be formed. Fig. 5 displays the growing trend of the number of particles with the oxygen concentration at each pool dimension (Fig. 5a) diameter and temperature (Fig. 5b); in addition, two more insights may be drawn from the plot: a stronger correlation of N_{0D} with O_2 fraction than with Na-vaporization rate (i.e., higher sensitivity of N_{0D} to X_{O2}) and the much larger scattering caused by other variables. In order to better illustrate the influence of pool diameter and temperature, Fig. 6 plots the specific variations of N_{0D} with both variables in the 21% O_2 scenario (the rest of cases showing the same trends). In short, whereas T_{pool} slightly affects the number of particles in the range explored, d_{pool} changes have a quite noticeable effect that might fit a potential relation with N_{0D}.

As for the primary particle diameter trends as a function of main variables, the study is simpler due to the small sensitivity shown by the

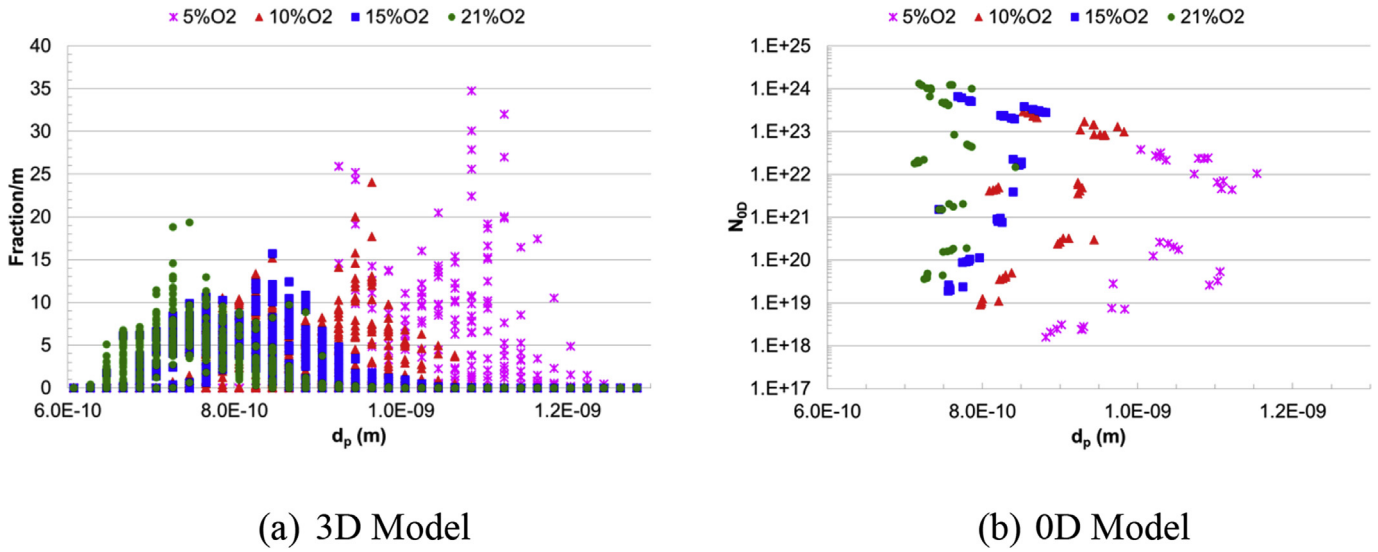

Fig. 3. Primary particle diameter.

model (range between $7{\cdot}10^{-10}$ and $1.2{\cdot}10^{-9}$ m). Hardly any variation has been found as a function of T_{pool} and d_{pool}, whereas oxygen concentration clearly shows an inverse relation between both variables (Fig. 7): the higher the O_2 concentration, the smaller the particle primary size. This trend is again consistent with the fact that higher Na_xO_y vapour pressures translate into smaller primary sizes according to the Classical Nucleation Theory (Becker and Döring, 1935; Farkas, 1927; Zeldovich, 1942).

Based on the individual trends presented above, N_{0D} has been linearly correlated with the vaporization rate and potentially correlated with the pool diameter and the oxygen concentration:

$$N_{crltn} = 7.8478{\cdot}10^{26}{\cdot}\dot{m}_{Na}{\cdot}d_{pool}^{0.22}{\cdot}X_{O_2}^{3.03} \quad (7)$$

Fig. 8 displays the correlation predictions vs. those from the 0D model. The correlation shows quite good behaviour with an average relative deviation around 50%. Garcia et al. (2016) estimated that just by considering the uncertainties affecting the physical properties intervening in the nucleation modelling a 2-orders-of-magnitude uncertainty band should be anticipated in the calculation of particle number. Therefore, the deviations incurred by the correlation proposed are acceptable.

Given the narrow interval found by the 3D model concerning primary particle diameter ($7.0{\cdot}10^{-10}$ – $1.2{\cdot}10^{-9}$ m), the derivation of an accurate correlation is not that important. Nonetheless, the weak dependencies on pool diameter and temperature and the stronger decreasing effect of O_2 concentration observed above have been encapsulated in the following expression:

$$d_{Pcrltn} = 1.5913{\cdot}10^{-10}{\cdot}d_{pool}^{0.0239}{\cdot}\ln\left(\frac{1}{X_{O_2}}\right){\cdot}\frac{1}{T_{pool}^{0.2281}} \quad (8)$$

In Fig. 9 the primary particle diameter given by the correlation is compared with the primary particle size by the 0D PG model; even though the correlation tends to underestimate the model predictions, the absolute average relative deviation is less than 18%. Anyway, the narrow diameter interval and the expected uncertainties affecting any calculated size make a primary particle diameter of 10^{-3} μm a reasonable assumption for Na-based particle generation modelling.

3. Assessment of the CPA* Module

The correlations proposed in the previous section have been

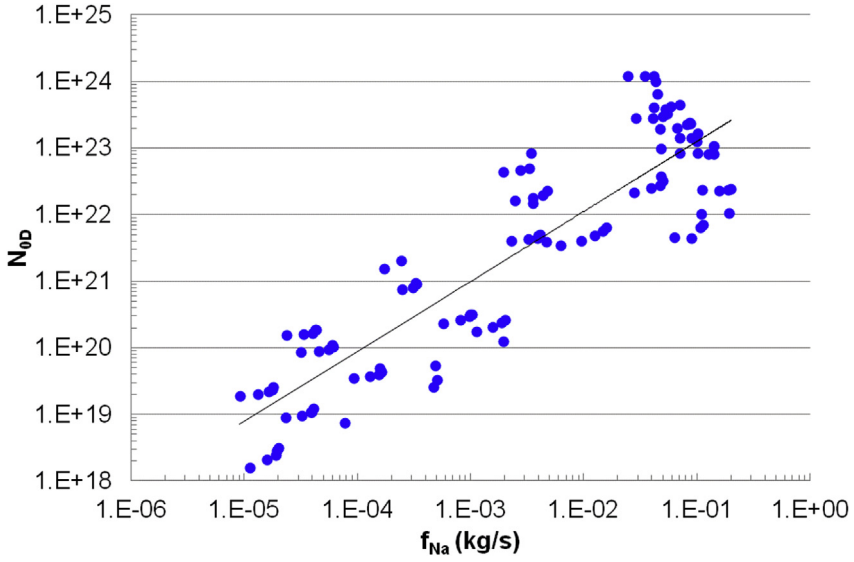

Fig. 4. N_{0D} as a function of Na-vaporization rate.

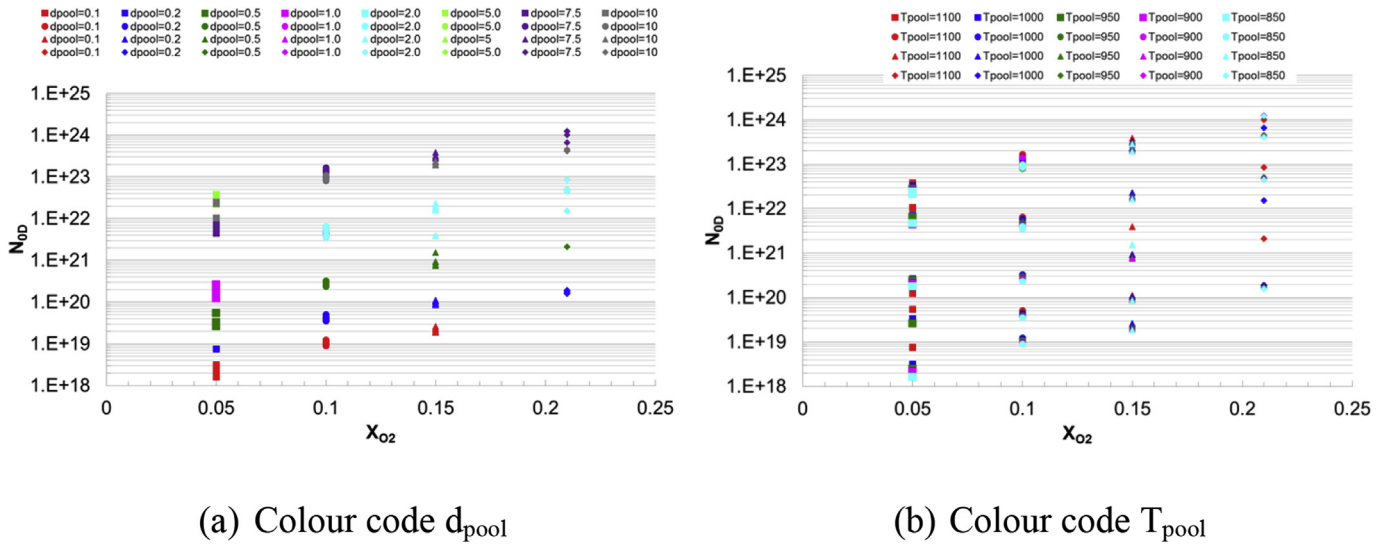

Fig. 5. N_{0D} as a function of O_2 concentration.

implemented within the CPA module of the ASTEC-Na code (Girault et al., 2015, 2017) together with a highly parametrized modelling approach (Herranz et al., 2017). The resulting version of CPA is hereafter referred to as CPA*. Next the code performance with the PG correlations is compared to experimental data (the existing pool-fire code option is also included for comparison).

3.1. Implementation of Zero-D correlations in CPA*

The new CPA version (CPA*) includes two options for the particle production from sodium pool fires: a sodium pool fire model based on the SOFIRE code formulation (Beiriger et al., 1973) in which sodium burning rate is limited by the diffusion of oxygen into the pool (surface reaction) and particle generation is assumed as infinitely fast or immediate; and the correlations derived from the 0D adaptation of the PG model assembled by Garcia et al. (2016), which is based on Na vapour gas-phase reactions (flame sheet approach) and the particle formation kinetics according to the Classical Nucleation Theory and the subsequent Na-oxide vapour condensation onto particle seeds.

The implementation of the correlations proposed in Eqns. (7) and (8) demands some additional information, like the sodium vaporization molar flow rate, which was derived by Garcia et al. (2016) assuming a diffusion layer approach:

$$\dot{M}_{Na} = \frac{D_{Na}\cdot X_{Na}\cdot C_{bl}\cdot \ln\left(\frac{P}{P-P_{sat,Na}}\right)\cdot A_{pool}}{l_f} \tag{9}$$

where the flame temperature (T_f) needed to estimate D_{Na} and C_{bl} as well as the distance from the pool surface to the flame (l_f) are given by correlations obtained from the test matrix (Table 1):

$$T_f = T_{pool} + 1397.13\cdot X_{O_2} \tag{10}$$

$$l_f = 1.061\cdot 10^{-16}\cdot \frac{1}{X_{O_2}^2}\cdot \exp(0.026163\cdot T_{pool}) \tag{11}$$

The oxygen mass flow rate is calculated by assuming equal generation rates of the two Na-oxide species considered (Na_2O and Na_2O_2):

$$\dot{m}_{O_2} = X\cdot \dot{M}_{Na}\cdot M_{Na} \tag{12}$$

where X is the oxygen-sodium stoichiometric ratio.

The conversion from Na-particle number to mass is conducted by assuming that particles formed can be approximated as spheres:

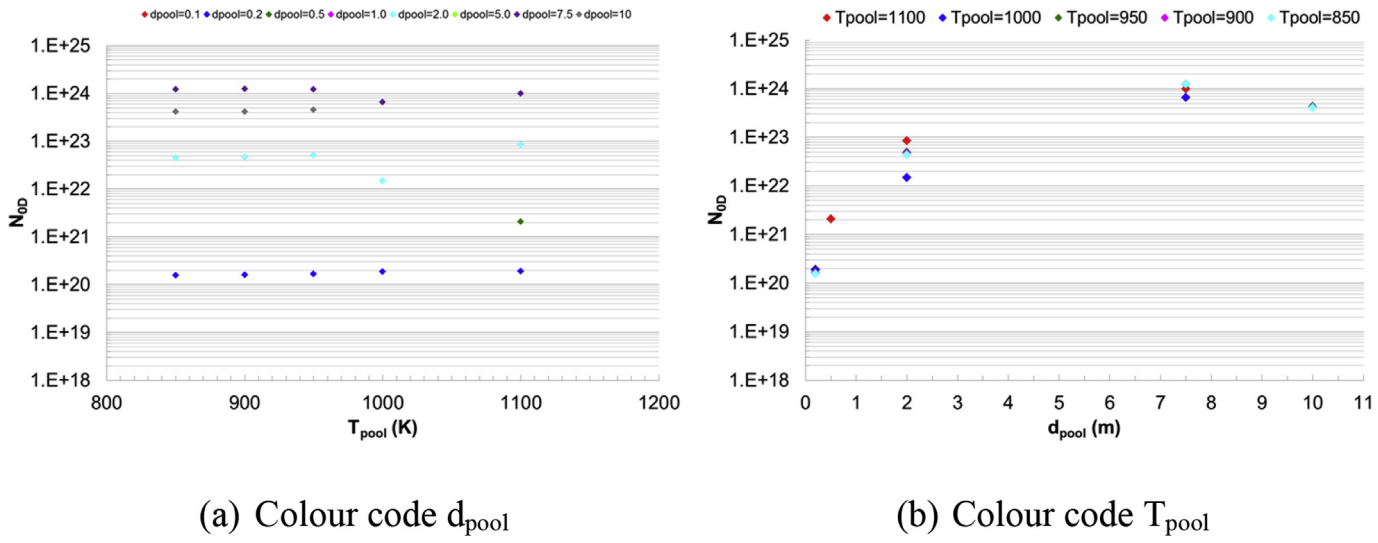

Fig. 6. N_{0D} variation as a function of T_{pool} and d_{pool} for the 21% O_2 scenario.

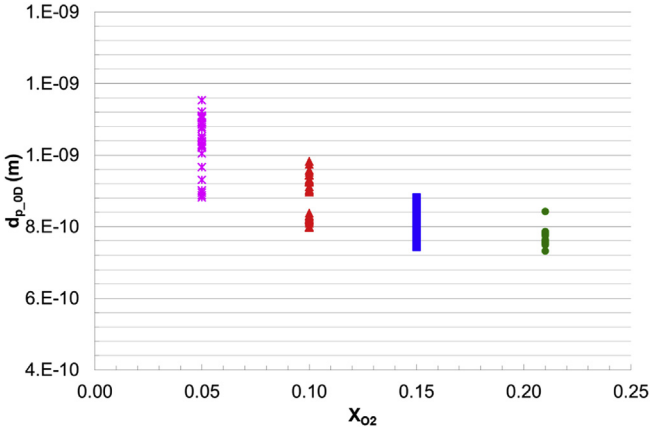

Fig. 7. d_{p_0D} as a function of oxygen fraction with pool diameter.

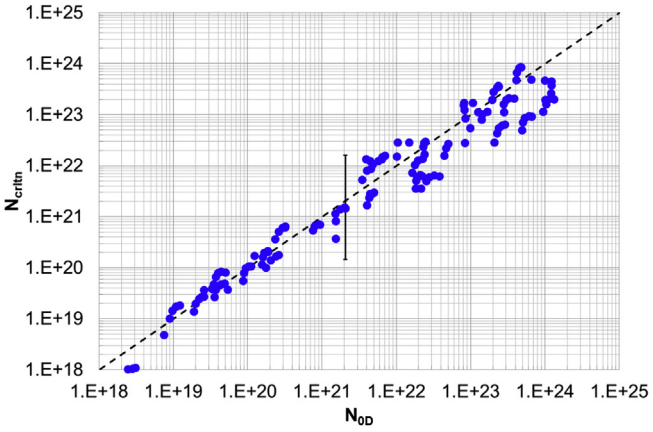

Fig. 8. Particle generation rate (correlated vs. 0D PG model results).

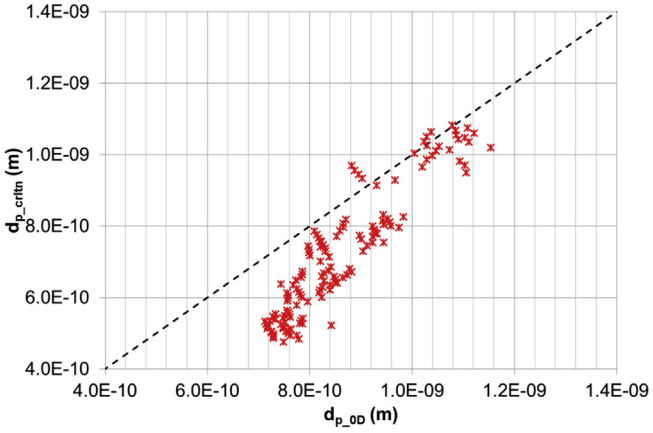

Fig. 9. Primary particle diameter (correlated vs. 0D PG model results).

$$\dot{m}_{Na,PG} = \frac{\dot{N}_{crltn}\frac{\pi}{6}d^3_{p_{crltn}}\rho_{aero}}{1.52} \tag{13}$$

where ρ_{aero} is a constant density specified by the user for the aerosol behaviour calculations according to the multi-component aerosol approach of ASTEC CPA (Bestele and Klein-Heßling, 2000). The value 1.52 comes from assuming that Na-oxides generation is equimolar.

The generated aerosol mass of Na_2O and Na_2O_2 is then calculated by the code:

$$\dot{m}_{Na_2O} = 0.673 \cdot \dot{m}_{Na,PG} \tag{14}$$

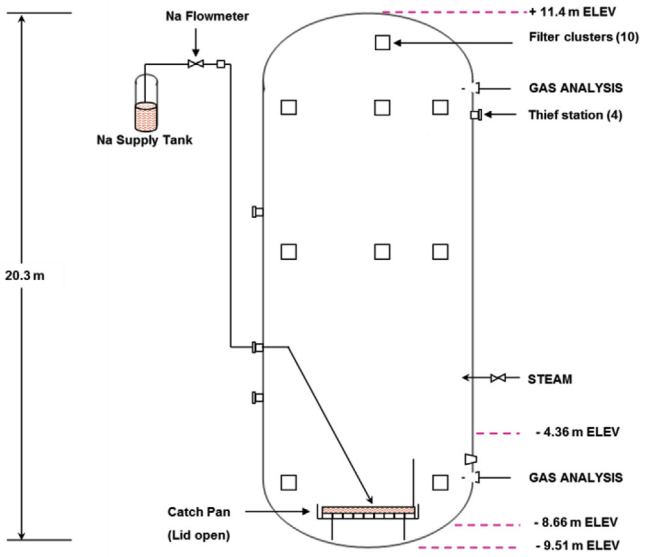

Fig. 10. CSTF vessel arrangement (Hilliard et al., 1977).

$$\dot{m}_{Na_2O_2} = 0.848 \cdot \dot{m}_{Na,PG} \tag{15}$$

3.2. Validation test matrix

Nearly 20 experiments related to Na fires were identified in Herranz et al. (2012). From them, almost half dealt with aerosol generation from pool fires. Based on a number of criteria like their scale, completeness and accuracy of data reported, two large-scale experiments from the ABCOVE programme (AB1 and AB2 tests) and one middle-scale experiment from FAUNA programme (F2 test) were chosen for the assessment of the new version of ASTEC-Na CPA code with the implemented PG model.

The ABCOVE experiments were conducted in the Containment System Test Facility (CSTF) vessel at the HEDL (Hanford Engineering Development Laboratory, USA) (Fig. 10). In test AB1, 410 kg of sodium at 600 °C was spilled into a burn pan of 4.4 m^2 through an electrically-heated delivery line. The burn pan had a hinged lid which was in the vertical position during the spill. The sodium flow lasted 80 s and the splashing was minimized by baffles in the pan. At 60 min after the initiation of the spill, the lid was closed and the sodium pool fire extinguished. The AB2 test was performed with essentially the same initial conditions, but with the addition of an injection of steam, at a rate of 0.02 kg/s, near the centre of the containment vessel, 16 min after the start of the fire. The steam injection was meant to simulate the release of water vapour from heated concrete at a rate equivalent to the release of water vapour from ~ 10–30 m^2 of hot concrete. In this test, 472 kg of sodium at 600 °C were delivered and the pool fire burn duration was 60 min. A more thorough description of experimental aspects may be found in Hilliard et al. (1979, 1977), McCormack et al. (1978) and Souto et al. (1994).

The FAUNA facility consists of a fire room, a measuring room, and an aerosol measuring loop. A cylindrical steel vessel of 6 m in diameter and 6 m high with domed ends (volume 220 m^3) served as the fire room (Fig. 11) with all the instrumentation needed to monitor both thermal-hydraulics and aerosol behaviour. Inside the FAUNA containment vessel, sodium pool fire was produced in a circular burning pan. Closely above the burning area a hood was placed in order to draw aerosols into the measurement loop. At these sample ports mass concentration of aerosol was determined by filter probes and size distribution by impactors. Additional filter probes were taken for the wet chemical

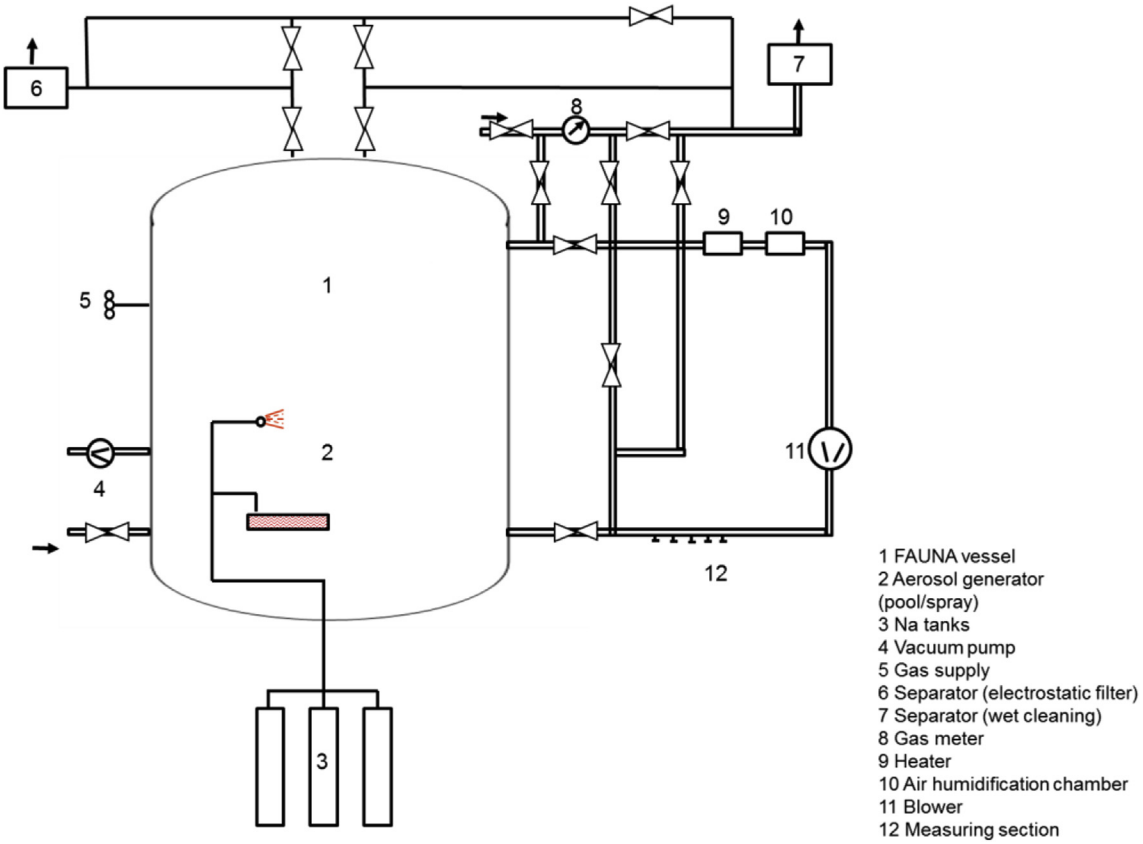

Fig. 11. FAUNA overview (Cherdron et al., 1985).

analysis (Cherdron et al., 1990; Cherdron and Charpenel, 1985; Cherdron and Jordan, 1980, 1983).

In the F2 test, a sodium pool fire was produced inside the FAUNA containment in a circular burning pan of 1.6 m diameter (~2 m^2) by the release of 250 kg of sodium at 500 °C for more than 3 h (210 min). During the experiment, the oxygen content was kept constant through 3 injections of approximately 1% of the vessel molar content with different duration.

In the next table an overview of the simulated experiments is shown (Table 2).

3.3. Results and discussion

Comparisons of CPA* to data are shown below in terms of atmosphere temperature, airborne aerosol concentration and size along time. A thorough description of data evolution and behaviour of heavily parametrized models in previous versions of ASTEC-Na were already reported by Herranz et al. (2017), so that the discussion below focuses on the new comparisons to data.

Table 2
Experiments overview.

	AB1	AB2	F2
Geometry			
Type	Cylindrical	Cylindrical	Cylindrical
Volume (m^3)	852	852	220
Initial Conditions			
O2 (%)	19.8	20.9	17–25
Temperature (K)	299.65	293.65	298.15
RH (%)	35.5	43.3	–
Steam Addition	NO	YES	YES
Sodium Spill			
Initial Na Temp. (K)	873.15	873.15	773.15
Burning Area (m^2)	4.4	4.4	2
Fire duration (s)	3600	3600	12,600

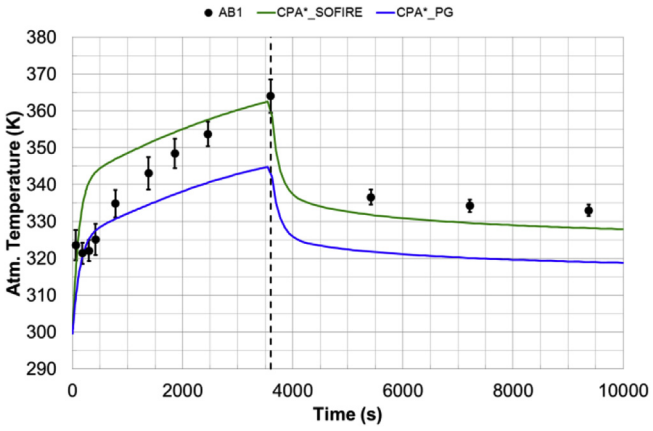

Fig. 12. Atmosphere temperature in AB1.

As observed in Fig. 12 through 14, calculated results and data roughly follow the same thermal trends by describing a heat-up phase, in which Na oxidation is taking place, and a cooling phase, in which the Na fire extinguishes and a fast cooldown period right after the fire is over, which is then followed by a moderate cooling governed by natural convection. This profile is somewhat distorted in the case of the F2 experiment for two main reasons: the F2 atmosphere was not well mixed during Na burning and temperature at the central axis of the vessel (x = 0.0 m) became highly sensitive to O_2 concentration, so that whenever O_2 concentration decreased temperature fell noticeably; in addition, even though the fire end was set at 12,600 s in the test protocol, according to temperature data, fire was progressively extinguishing from around 6000 s, which might have been caused by a slow supply of O_2 by the convection loops set in the vessel with respect to the

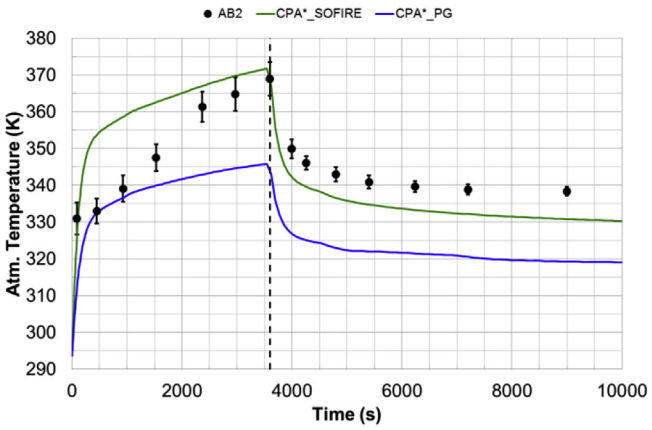

Fig. 13. Atmosphere temperature in AB2.

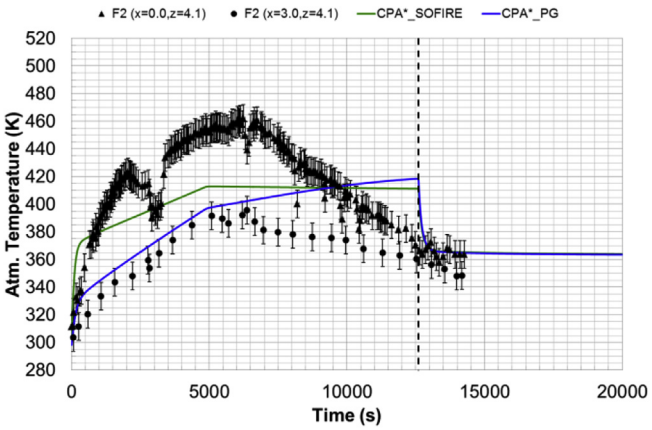

Fig. 14. Atmosphere temperature in F2.

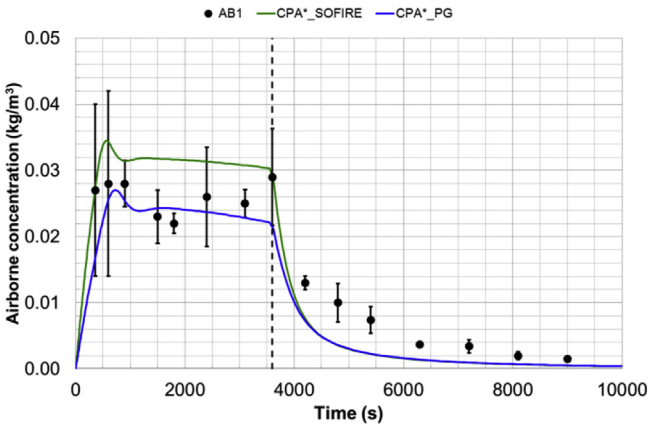

Fig. 15. Airborne concentration in AB1.

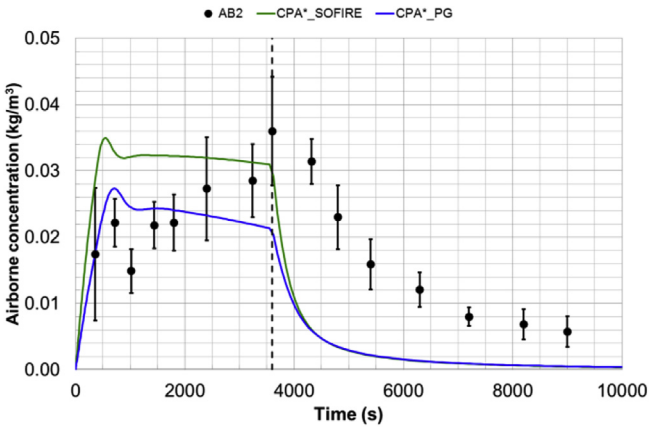

Fig. 16. Airborne concentration in AB2.

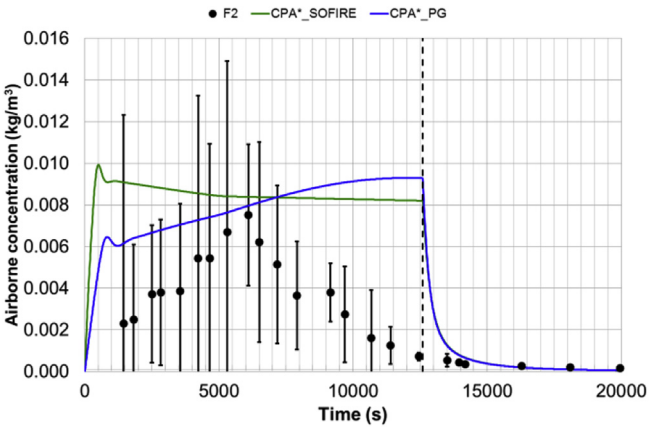

Fig. 17. Airborne concentration in F2.

Na burning rate at the measurement locations. As for the specific CPA*_PG behaviour, it closely captured the first 500 s of Na fires (AB1 and AB2 tests), but then it underestimated temperature data during the heat-up phase. This might indicate that either more chemical energy should have been released or a larger fraction of the chemical energy produced should remain in the atmosphere. Given the validation of the 3D PG model by Garcia et al. (2016) in terms of burning rate with Newman's data and the assumption of instantaneous chemical reaction, this might indicate a slight underprediction of the Na vaporization rate when converting Eqn. (9) into an adapted version for lumped-parameter codes. However, the similarity of the CPA*_SOFIRE slope during most of heat-up phase indicates that this is not strictly linked to the PG adaptation modelling (the apparently closer agreement of CPA*_SOFIRE with data at later times during the heat-up phase coming from the noticeable overprediction in the first 500 s of the test). During the cooling phase, the CPA*_PG behaves similarly to data, although the fast temperature decrease right after Na fire is slightly more moderate possibly due to the smaller temperature differences with surrounding heat structures as a consequence of the underestimate of gas temperature during the heat-up phase.

Much closer related to the PG modelling are the evolution of airborne aerosol concentration and size. Fig. 15 through 17 present the CPA*_PG results together with data and CPA*_SOFIRE predictions for the three experiments. Due to the reasons given above, comparisons to data in the case of the F2 test will be restricted to the first 6000 s. In AB1 and AB2, CPA*_PG calculations show consistency with data until around 2000–2500 s, during which they are within the experimental uncertainties; however, if credit is given to the blurred increasing trend (large experimental uncertainties prevent firm acceptation that such a tendency is true), this might either support a higher Na vaporization rate, as explained above, or indicate over-efficient particle removal by the aerosol depletion mechanisms (mainly sedimentation). Anyway, the larger deviations found with respect to data are within a factor of 2.0 (CPA*_SOFIRE estimates behaved similarly but with a shift to higher aerosol concentrations that locates them beyond the experimental uncertainties during the early times of heat-up phase). As for the F2 experiment, the CPA*_PG calculations show a growing trend consistent with the data trend for the first 6000 s, although experimentally the sharp increase predicted at the beginning of the test (and also measured in AB1 and AB2) did not exist, which is likely related to the stratified atmosphere reported in the test. Once the Na fire is over, the particle generation model has no effect on aerosol evolution, so that

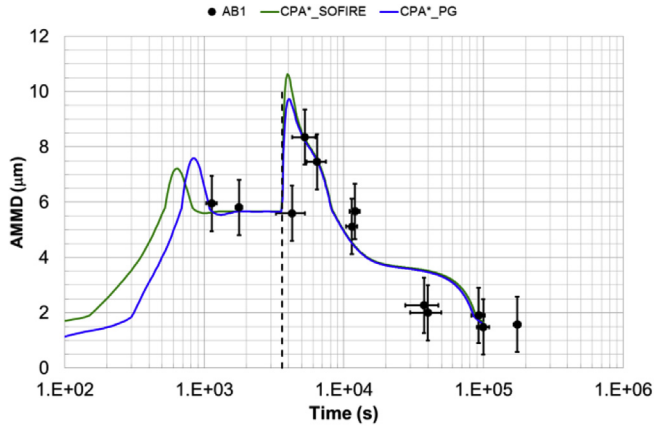

Fig. 18. AMMD in AB1.

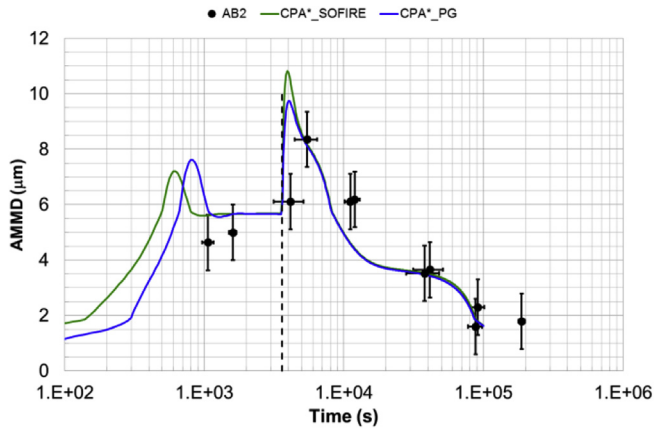

Fig. 19. AMMD in AB2.

discrepancies with data cannot be attributed to PG modelling.

Fig. 18 through 20 display the Aerosol Mass-Median Diameter (AMMD) evolution. Given the absence of data before 1000 s, no discussion can be held concerning the earlier times of the heat-up phase except for stating that particle growth predicted by both CPA* approximations are consistent with the data available (Figs. 18 and 19). This is particularly so in the AB1 test, in which a steady state is observed in the AMMD until the fire end time; contrarily, in the AB2 test, a growth trend, not calculated by either of the CPA* calculations, might have existed, although again the experimental uncertainties do not allow confirmation of such a trend. Anyway, the comparisons support that CPA*_PG implementation does not distort the particle growth

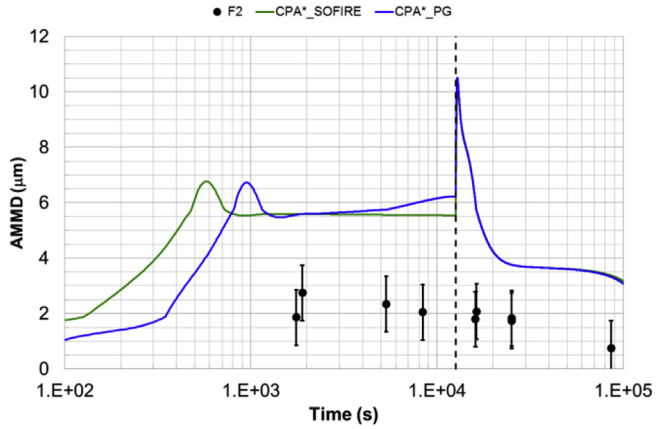

Fig. 20. AMMD in F2.

observed at two key times: early during the heat-up phase to roughly the measured diameter and then once the fire is over and particle generation is not active anymore, making predictions reproduce the particle size jump. Regarding F2, CPA*_PG noticeably overpredicted size; however, this is the expected behaviour because the measurements were made quite close to the aerosol source so that particles had a short "time of flight" (i.e., particle size practically unaffected by agglomeration processes); this explanation is consistent with steady behaviour observed from the data before and after the fire was put out, instead of producing a size jump due to the end of production of small particle injection in the vessel.

4. Conclusions

Sodium pool-fire modelling has traditionally focused on thermal-hydraulic consequences to evaluate the risk of containment overpressure. However, in the case of a core-damage accident and rupture of the primary system, fire-generated particles will not only be toxic but also represent the main vector of radio-contaminant transport. Here modelling of sodium-vapour burning and formation of sodium-oxide aerosols above an evaporating sodium pool has been presented with the objective of calculating the characteristics (number and size) of the particulate source term to the containment. Firstly, a 0D (lumped) model is derived from a previously-published 3D model; this 0D model is a first step towards a model suited to implementation in severe-accident codes. On the basis of realistic variations of burning-pool parameters (viz., gas-phase oxygen concentration, pool size and pool temperature), comparisons of the results of the 0D model and the 3D model are observed to be in acceptable agreement in terms of both the number of particles produced and their size. From further results of the 0D model, simple correlations for particle number and size are proposed in terms of the following pool-fire parameters: sodium evaporation rate; pool diameter; pool temperature and oxygen concentration. The implementation of these correlations into the ASTEC-Na severe-accident code is described where this is done in parallel (i.e., as a user-selectable alternative) to existing modelling for fire-particle generation. However, unlike the new modelling, the existing modelling imposes fixed particle size for the primary (freshly-nucleated) fire-generated particles. Calculated results using the new and existing particle-generation models are compared with experimental data from three experiments in two different facilities. Overall, the new modelling in ASTEC-Na does not provide better or worst results than alternate modelling. The trends have been proved to be physically sound (they follow data tendencies) and the experimental data uncertainty prevents from qualifying one approach over the other. This being said, the correlations proposed do not need any code-user assumption concerning the mass and energy transfer from a pool fire to the containment atmosphere, as other approaches do.

In conclusion, the new correlations are very suitable for use in a severe-accident code in terms of the negligible additional computation burden. The new correlations, by originating from simplifications of soundly-based physical modelling, avoid the arbitrary assumption of a fixed primary-particle size in the existing modelling. Limited comparisons with experiments imply that use of the new correlations increases confidence in prediction of the pool-fire particulate source term to the containment.

Acknowledgments

The CIEMAT authors wish to thank the JASMIN partners for the fruitful discussion held and the European Commission for partially funding the research presented in this paper (contract number 295803).

Nomenclature

A_{pool}	Na-pool surface
C_{bl}	molar gas concentration between pool surface and flame
D_{Na}	diffusivity of sodium in the binary system N_2—Na
d_{Pcrltn}	correlated particle diameter
d_{0D}	particle diameter in the 0D PG model
d_{pool}	Na-pool diameter
J_{CNT}	nucleation rate by Classical Nucleation Theory
k	Boltzmann constant
l_f	flame height
m_1	molecular mass
$\dot{m}_{Na}$	Na-vapour mass flow rate
$\dot{m}_{NaPG}$	Na mass flow rate into particles
$\dot{m}_{Na_2O}$	generated aerosol mass of Na_2O
$\dot{m}_{Na_2O_2}$	generated aerosol mass of Na_2O_2
$\dot{m}_{O_2}$	oxygen mass flow rate
M_{Na}	Na molar weight
$\dot{M}_{Na}$	Na-vapour molar flow rate
N_{crtl}	correlated number of generated particles
N_{3D}	number of generated particles calculated with the 3D PG model
N_{0D}	number of generated particles calculated with the 0D PG model
$\dot{N}_1$	average number concentration of molecules
P	pressure
$p_{sat,Na}$	saturation vapour pressure
p_{v_i}	cell vapour pressure
$\overline{p}_v$	average vapour pressure
S	saturation ratio
$\overline{S}$	average saturation ratio
$\overline{T}$	average temperature
T_f	flame temperature
T_i	cell temperature
T_{pool}	Na-pool temperature
v_i	cell volume
V_{PG}	nucleation zone volume
v_1	molecular volume
X_{Na}	fraction of sodium on the pool surface
X_{O2}	fraction of oxygen

Greek symbols

ρ_{aero}	aerosol density
σ	surface tension

References

ANSYS Inc, 2008. FLUENT computational Fluid Dynamics Software. FLUENT User's Guide.

Baskaran, R., Subramanian, V., Venkatraman, B., Chellapandi, P., 2011. Sodium aerosol studies for fast reactor safety. Energy Proc. Asian Nuclear Prospect. 7, 660–665. https://doi.org/10.1016/j.egypro.2011.06.089.

Becker, R., Döring, W., 1935. Kinetische Behandlung der Keimbildung in übersättigten Dämpfen. Ann. Phys. 416, 719–752. https://doi.org/10.1002/andp.19354160806.

Beiriger, P., Hopenfeld, J., Silberberg, M., Johnson, R.P., Baurmash, L., Koontz, R.L., 1973. Sofire II User Report (No. AI-aec–13055). Atomics International, Canoga Park, Calif. (USA).

Bestele, J., Klein-Heßling, W., 2000. ASTEC V0 CPA Module Containment Thermalhydraulics and Aerosol and Fission Product Behaviour User Guidelines. No. ASTEC-V0/DOC/00-14, GRS.

Cherdron, W., Bunz, H., Jordan, S., 1985. Properties of sodium fire aerosols and re-calculation of their behaviour in closed containments. In: Presented at the CSNI Specialist Meeting on Nuclear Aerosols in Reactor Safety, CSNI-95, Karlsruhe, pp. 395–405.

Cherdron, W., Charpenel, J., 1985. Thermodynamic Consequences of Sodium spray Fires in Closed Containments. Pt. 2 (No. KFK–3831). Kernforschungszentrum Karlsruhe G.m.b.H. Laboratorium für Aerosolphysik und Filtertechnik, Germany.

Cherdron, W., Jordan, S., 1983. Die Natrium-Brandversuche in der FAUNA-Anlage auf Brandflächen bis 12m2 (No. KfK 3041). Kernforschungszentrum Karlsruhe G.m.b.H. Laboratorium für Aerosolphysik und Filtertechnik, Germany.

Cherdron, W., Jordan, S., 1980. Determination of sodium fire aerosol process coefficients from FAUNA-experiments. In: NUREG/CR-1724. Presented at the CSNI Specialist Meeting on Nuclear Aerosols in Reactor Safety, CSNI-45, Gatlingburg, Tennessee (USA), pp. 129–138.

Cherdron, W., Jordan, S., Lindner, W., 1990. Die Natriumbrand-Untersuchungen in der FAUNA: Poolbrände und Aerosolverhalten (No. KfK 4358). Kernforschungszentrum Karlsruhe G.m.b.H 1990, Laboratorium für Aerosolphysik und Filtertechnik, Germany.

Farkas, L., 1927. Keimbildungsgeschwindigkeit in übersättigten Dämpfen. Phys. Chem. 125, 239.

Garcia, M., Herranz, L.E., Kissane, M.P., 2016. Theoretical assessment of particle generation from sodium pool fires. Nucl. Eng. Des. 310, 470–483. https://doi.org/10.1016/j.nucengdes.2016.10.024.

Girault, N., Cloarec, L., Herranz, L.E., Bandini, G., Perez-Martin, S., Ammirabile, L., 2015. On-going activities in the European JASMIN project for the development and validation of ASTEC-Na SFR safety simulation code. In: ICAPP2015. Presented at the International Congress on Advances in Nuclear Power Plants (ICAPP 2015), Nice (France), pp. 482–494.

Girault, N., Cloarec, L., Lebel, L., 2017. Main outcomes from the JASMIN project: development of ASTEC-Na for severe accident simulation in Na cooled fast reactors. In: Presented at the International Conference on Fast Reactors and Related Fuel Cycles: Next Generation Nuclear Systems for Sustainable Development (FR17), Yekaterinburg (Russia).

Herranz, L.E., Garcia, M., Kissane, M.P., 2012. In-containment source term in accident conditions in sodium-cooled fast reactors: data needs and model capabilities. Prog. Nucl. Energy 54, 138–149. https://doi.org/10.1016/j.pnucene.2011.07.003.

Herranz, L.E., Garcia, M., Lebel, L., Mascari, F., Spengler, C., 2017. In-containment source term predictability of ASTEC-Na: major insights from data-predictions benchmarking. Nucl. Eng. Des. 320, 269–281. https://doi.org/10.1016/j.nucengdes.2017.06.010.

Hilliard, R.K., McCormack, D., Postma, A.K., 1979. Aerosol Behavior during Sodium Pool Fires in a Large Vessel - CSTF Tests AB1 and AB2 (No. HEDL-TME 79-28). Hanford Engineering Development Lab.

Hilliard, R.K., McCormack, J.D., Hassberger, J.A., Muhlestein, L.D., 1977. Preliminary Results of CSTF Aerosol Behavior Test, AB1. [LMFBR] (No. HEDL-SA-1381).

Lee, Y.B., Choi, S.K., 1997. A study on the development of advanced model to predict the sodium pool fire. J. Korean Nucl. Soc. 29, 240–250.

Lhiaubet, G., Bunz, H., Kissane, M.P., Seino, H., Miyake, O., Himeno, Y., Casselman, C., Such, J.M., Rzekiecki, R., 1990. Comparison of aerosol behavior codes with experimental results from a sodium fire in a containment. In: EUR 12374, 1991. Presented at the International Fast Reactor Safety Meeting. American Nuclear Society, American Nuclear Society, Snowbird, Utah.

Louie, D., Humphries, L.L., 2016. Melcor/contain Lmr Implementation Report - Fy16 Progress (No. SAND–2016-12101). Sandia National Laboratories (SNL-NM), Albuquerque, NM (United States). https://doi.org/10.2172/1334936.

Malet, J.C., Sophy, Y., Rzekiecki, R., Cucinotta, A., Mosse, D., 1990. Extensive sodium fire studies: general survey of the esmeralda programme results. In: Presented at the International Fast Reactor Safety Meeting, Snowbird, Utah.

McCormack, J.D., Hilliard, R.K., Postma, A.K., 1978. Recent Aerosol Tests in the Containment Systems Test Facility (No. HEDL-sa-1686). Hanford Engineering Development Lab., Richland, WA (USA).

Miyake, O., Miyahara, S., Ohno, S., Himeno, Y., 1991. Sodium pool combustion codes for evaluation of fast breeder reactor safety. J. Nucl. Sci. Technol. 28, 107–121. https://doi.org/10.1080/18811248.1991.9731330.

Murata, K.K., Carroll, D.E., Bergeron, K.D., Valdez, G.D., 1993. A Computer Code for Containment Analysis of Accidents in Liquid-metal Cooled Nuclear Reactors (No. SAND91-1490). Sandia National Labs., Albuquerque, NM (United States).

Newman, R.N., 1983. The ignition and burning behaviour of sodium metal in air. Prog. Nucl. Energy 12, 119–147. https://doi.org/10.1016/0149-1970(83)90020-3.

Newman, R.N., Payne, J.F.B., 1978. The burning rates of sodium pool fires. Combust. Flame 33, 291–297. https://doi.org/10.1016/0010-2180(78)90067-6.

Sagae, K., Suzuoki, A., 1985. Development of analytical model for sodium pool combustion. J. Nucl. Sci. Technol. 22, 870–880. https://doi.org/10.1080/18811248.1985.9735739.

Souto, F.J., Haskin, F.E., Kmetyk, L.N., 1994. Melcor 1.8.2 Assessment: Aerosol Experiments Abcove Ab5, Ab6, Ab7, and Lace La2 (No. SAND–94-2166). Sandia National Labs., Albuquerque, NM (United States).

Subramanian, V., Baskaran, R., 2007. Initial size distribution of sodium combustion aerosol. Nucl. Technol. 160, 308–313. https://doi.org/10.13182/NT07-A3901.

Subramanian, V., Sahoo, P., Malathi, N., Ananthanarayanan, R., Baskaran, R., Saha, B., 2009. Studies on chemical speciation of sodium aerosols produced in sodium fire. Nucl. Technol. 165, 257–269. https://doi.org/10.13182/NT09-A4100.

Takata, T., Yamaguchi, A., Maekawa, I., 2003. Numerical investigation of multi-dimensional characteristics in sodium combustion. Nucl. Eng. Des. 220, 37–50. https://doi.org/10.1016/S0029-5493(02)00232-7.

Yamaguchi, A., Tajima, Y., 2009. Sodium pool combustion phenomena under natural convection airflow. Nucl. Eng. Des. 239, 1331–1337. https://doi.org/10.1016/j.nucengdes.2009.04.004.

Yamaguchi, A., Tajima, Y., 2003. Validation study of computer code sphincs for sodium fire safety evaluation of fast reactor. Nucl. Eng. Des. 219, 19–34. https://doi.org/10.1016/S0029-5493(02)00209-1.

Zeldovich, J., 1942. Theory of the formation of a new phase, cavitation. Zh. Eksp. Theor. Fiz. 12, 525–538.